Designing Rainbow Metamaterials

H. Meng[1*] D. Chronopoulos[1*]

[1] University of Nottingham, Nottingham, UK
han.meng@nottingham.ac.uk, dimitrios.chronopoulos@nottingham.ac.uk,

Abstract. Nonperiodic metamaterials can have better vibration attenuation than periodic metamaterials with properly designed resonator distributions. In this study, we propose optimal design routes for rainbow metamaterials. The rainbow metamaterials are nonperiodic structures that are composed of Π-shaped beams as backbones and attached spatially varying cantilever-mass resonators. The main optimization objective is to obtain good vibration attenuation within frequency of interests. Frequency response functions of the rainbow metamaterials are first calculated by an analytical model that is built on the basis of the displacement transfer matrix method. Two optimization objective functions are developed with the maximum and average receptance values within a prescribed frequency range respectively. The mass of resonators acts as design variables. The objective functions are later solved by virtue of the Genetic Algorithm method. The optimized rainbow metamaterials show good vibration attenuation in the prescribed optimization frequency range.

Keywords: Rainbow metamaterial, Optimization, Vibration attenuation, Genetic Algorithm.

1 Introduction

Metamaterials are a new class of artificial composites engineered to have transcendental properties that cannot found from natural materials. In the past decades, metamaterials have attracted much attention in many research fields. Metamaterials are originally introduced to tailor the electromagnetic optical waves [1-4]. Nowadays, the concept of metamaterial has expanded to the areas of acoustic/elastic metamaterials. Unusual properties such as negative effective mass and dynamic stiffness [5] and negative bulk modulus [6] can be seen from elastic/ acoustic metamaterials.

An important feature of elastic/acoustic metamaterials is the existence of bandgaps within which no waves can propagate. Locally resonant bandgaps rely on the resonance of internal oscillators, hence generally happen at low frequencies. Henceforth, a lot of elastic/acoustic metamaterial have been proposed with various local resonators, such as inclusions coated with soft rubber [5], Helmholtz resonator [7], cantilever beam resonator [8] and membrane with attached mass [9].

Most of the proposed metamaterials are periodic structures. Several designs have been recently investigated [10-14]. Nonetheless, although these periodic metamaterials

are applicable for manipulating wave propagation and providing low-frequency vibration attention, broad bandgaps are hard to be achieved. Few researchers presented the nonperiodic metamaterials with spatially varying resonators. Sun *et al*. [15] and Pai [16] made the first attempt at investigating metamaterials with spatially varying mass-spring-damper subsystems. Their investigations proved that metamaterials with properly designed spatially varying resonators can achieve better vibration attenuation than that with periodic resonators. Nonetheless, there are no existing research that studied systematically the nonperiodic metamaterials or proposed optimal design routes for the nonperiodic metamaterials.

In the present manuscript, we first put forward a design approach for the distributions of resonators in nonperiodic metamaterials. A nonperiodic elastic metamaterial that is constructed by Π-shaped beams with rainbow-shaped cantilever-mass resonators is developed in the present paper. An analytical model is first proposed to solve the frequency response functions of the rainbow metamaterial. The analytical model is later validated by comparison with experimental results. After that a genetic algorithm optimization method is applied to search the optimal nonperiodic distributions of resonator mass that can generate best receptance values within prescribed frequency range.

2 Analytical modelling method for the rainbow metamaterial

An analytical model is employed to determine the structural dynamics of the rainbow metamaterial [17-18]. Figure 1(a)-(c) shows the schematic diagram of the proposed rainbow metamaterial. The Π-shaped beam is partitioned into subspaces by periodic plate insertions. Cantilever-mass subsystems are clamped to the two side walls of the Π-shaped beam in each subspace.

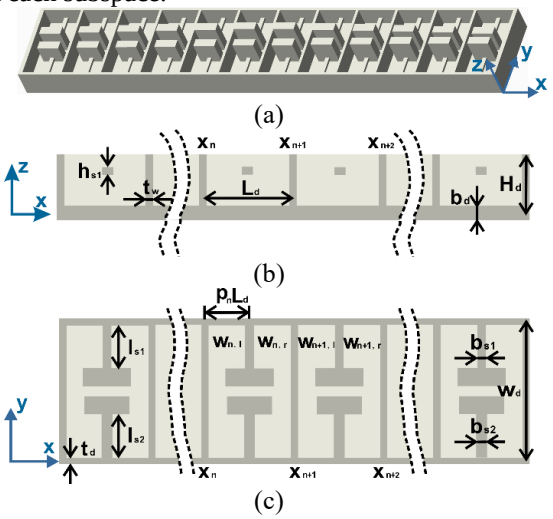

Fig.1. Schematic diagram of the rainbow metamaterial (a) global view, (b) side view, (c) top view

Assuming a finite metamaterial is of free-free boundary and subjected to an excitation at one end, given the equilibrium conditions, governing equations at the two ends are,

$$\begin{aligned} F + m_f \omega^2 W_{1,l}\big|_{x=0} &= EI_z W_{1,l}'''\big|_{x=0} \\ -J_f \omega^2 W_{1,l}'\big|_{x=0} &= EI_z W_{1,l}''\big|_{x=0} \\ EI_z W_{q,r}'''\big|_{x=L} + m_f \omega^2 W_{q,r}\big|_{x=L} &= 0 \\ EI_z W_{q,r}''\big|_{x=L} - J_f \omega^2 W_{q,r}'\big|_{x=L} &= 0 \end{aligned} \tag{1}$$

The displacement transfer matrix between the nth and $(n+1)$th segments of the metamaterial beam is given as

$$\begin{bmatrix} \alpha_{n+1,l} \\ \beta_{n+1,l} \\ \chi_{n+1,l} \\ \varepsilon_{n+1,l} \end{bmatrix} = \mathbf{R}^{-1}\mathbf{U}\boldsymbol{\Lambda}_{n,r} \begin{bmatrix} \alpha_{n,r} \\ \beta_{n,r} \\ \chi_{n,r} \\ \varepsilon_{n,r} \end{bmatrix} \tag{2}$$

where $\mathbf{R}$, $\mathbf{U}$

$$\begin{aligned} \boldsymbol{\Lambda}_{n,r} &= \mathrm{diag}\left(e^{-ik(1-p_n)L_d}, e^{-k(1-p_n)L_d}, e^{ik(1-p_n)L_d}, e^{k(1-p_n)L_d}\right) \\ \mathbf{R} &= \begin{bmatrix} 1 & 1 & 1 & 1 \\ -i & -1 & i & 1 \\ -EI_z k^2 & EI_z k^2 & -EI_z k^2 & EI_z k^2 \\ iEI_z k^3 & -EI_z k^3 & -iEI_z k^3 & EI_z k^3 \end{bmatrix} \\ \mathbf{U} &= \begin{bmatrix} 1 & 1 & 1 & 1 \\ -i & -1 & i & 1 \\ \left(-EI_z k^2 + iJ_f \omega^2 k\right) & \left(EI_z k^2 + J_f \omega^2 k\right) & \left(-EI_z k^2 - iJ_f \omega^2 k\right) & \left(EI_z k^2 - J_f \omega^2 k\right) \\ \left(iEI_z k^3 + m_f \omega^2\right) & \left(-EI_z k^3 + m_f \omega^2\right) & \left(-iEI_z k^3 + m_f \omega^2\right) & \left(EI_z k^3 + m_f \omega^2\right) \end{bmatrix} \end{aligned} \tag{3}$$

The receptance function of the rainbow metamaterial is derived by combing the boundary conditions of the finite beam in Eq. (1) and transfer matrix in Eq. (2),

$$R_{ec} = 20\log_{10}\left|\frac{w_{m,r}\big|_{x=L}}{F}\right| \tag{4}$$

3 Experimental validation

The analytical model is verified by comparing with the experimental results. The tested samples are fabricated by additive manufacturing method. The receptance function of printed samples are measured by receptance measuring system as shown in Fig. 2.

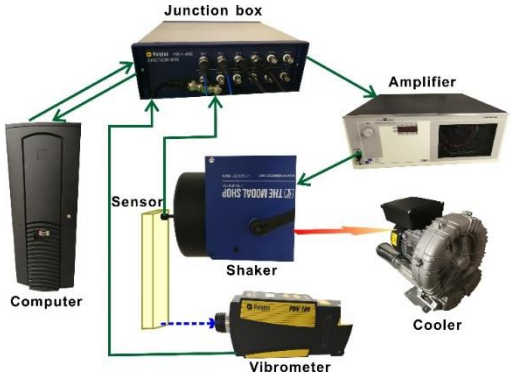

Fig. 2. Experimental setup for receptance tests of the rainbow metamaterials

Comparison between the experimental and analytical results are shown in Fig. 3. It can be seen that the experimental results are in agreement with the estimated results by analytical model.

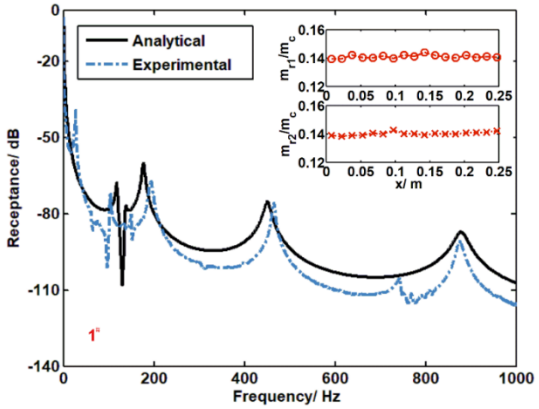

Fig. 3. Amplitude of transfer receptance comparison between analytical (—) and experimental (---) results

4 Optimization strategy

Since the frequency functions of the rainbow metamaterials are greatly affected by the distributions of resonator mass, we thus assign the resonator mass as design variables to achieve effective vibration attenuation by virtue of rational optimization strategy as shown in Fig. 4.

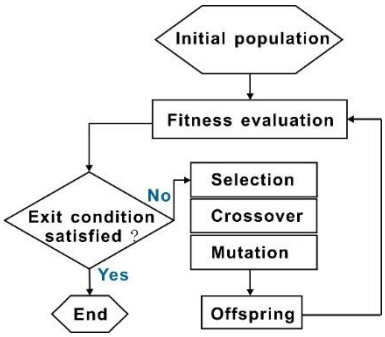

Fig. 4. Flowchart of Genetic Algorithm optimization process.

In order to maximize the vibration attenuation by the local resonators in a prescribed frequency range, two optimization strategies are proposed that invoke two objective functions individually.

One of the objective functions is set based on the maximum receptance value within the prescribed frequency ranges, written as

$$\min \quad \max\left(R_{ec}\left(\mathbf{M}_1, \mathbf{M}_2, \mathbf{\Phi}\right)\right) \tag{5}$$

where $\mathbf{M}_1 = \left(m_{11}, m_{12}, ..., m_{1t}\right)$ and $\mathbf{M}_2 = \left(m_{21}, m_{22}, ..., m_{2t}\right)$ represent the mass of resonators at different sides of the complex beam, $\mathbf{\Phi} = \left(f_1 \sim f_2\right)$ is the prescribed frequency regime. Receptance within the prescribed frequency range are destined to be low when the maximum value remains minimal, the vibration attenuation is thus optimized.

Constrains of the design variables are given as,

$$\begin{aligned} s.t. \quad & m_{1i} = m_{2i} \\ & m_{11}, m_{12}, ..., m_{1t} \geq 0 \\ & 2\sum_i m_{1i} \leq 0.3M \\ & i = 1, 2, ..., t \end{aligned} \tag{6}$$

Average value is another evident assessment criteria of the receptance within a prescribed frequency range, therefore, the other objective function is set up based on the average receptance value within the prescribed frequency range, written as

$$\min \quad \frac{\int_{\mathbf{\Phi}} R_{ec}\left(A, B, C, D, \mathbf{\Phi}\right) df}{f_2 - f_1} \tag{7}$$

The constrains of design variables are the same as shown in Eq. (6).

5 Optimization example

Assuming the prescribed single frequency range is 130-150 Hz. As discussed in Sections 4, two objective functions are defined, hence two fitness functions are applicable

for the GA optimization process as shown in Fig. 4. Receptance values of the two rainbow metamaterials with optimal resonator mass distributions are compared with that of complex beams of the same mass but without resonators in Figs. 5 and 6 respectively. The optimal rainbow metamaterials in Figs. 5 and 6 are obtained by the maximal receptance value based objective function and average value based objective function respectively. As it can be seen, both of the two optimal rainbow metamaterials show bandgaps within the prescribed frequency range, the receptance values are hence greatly reduced. The optimal metamaterial in Fig. 5 has a maximal receptance about 38 dB less than that of the structure without resonators, while the average receptance difference between the optimal structure and the no-resonator beam in Fig. 6 is about 33 dB, that is, both maximum and average displacements within 130~150 Hz can be reduced by a factor of more than 70 with the optimization process.

Besides, it also can be seen from Figs. 5 and 6 that the optimal structure by maximum value based objective function has broader bandgap but bigger receptance value within the prescribed frequency range, which is opposite to the optimal structure derived by average value based objective function. Optimization strategy can be chosen according to requirements of different applications.

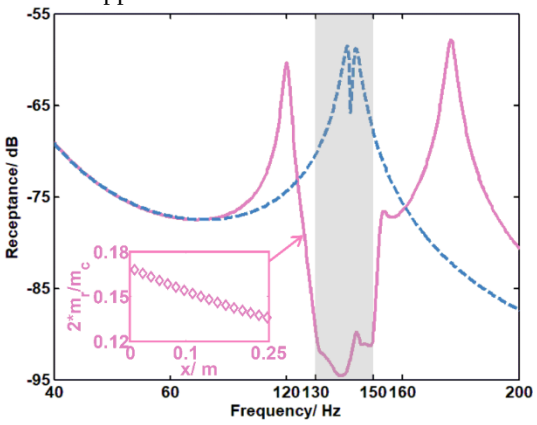

Fig. 5. Receptance comparison between optimal rainbow metamaterial by maximal value based objective function and no-resonator complex beam

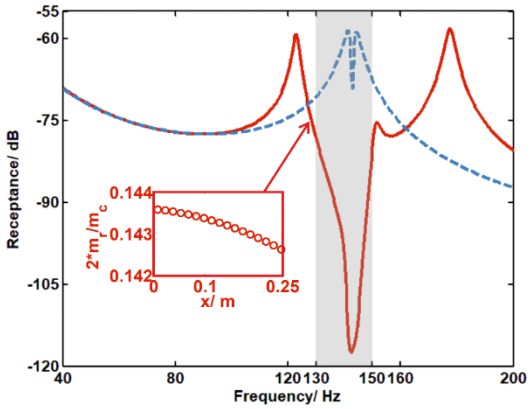

Fig. 6. Receptance comparison between optimal rainbow metamaterial by average value based objective function and no-resonator complex beam

Acknowledgements

We would like to acknowledge the support acquired by the H2020 DiaMoND project (Grant Agreement ID:785859), Royal Society Grant: PURSUIT, the Brazilian National Council of Research CNPq (Grant Agreement ID: 420304/2018-5) and the Brazilian Federal District Research Foundation (Grant Agreement ID: 0193.001507/2017).

References

1. J.B. Pendry, Negative Refraction Makes a Perfect Lens, *Physical Review Letters*, 85, 3966-3969 (2000).
2. J.B. Pendry, Negative refraction, *Contemporary Physics*, 45, 191-202 (2004).
3. R.A. Shelby, D.R. Smith, S. Schultz, Experimental verification of a negative index of refraction, *Science*, 292, 77-79 (2001).
4. T. Tanaka, A. Ishikawa, S. Kawata, Unattenuated light transmission through the interface between two materials with different indices of refraction using magnetic metamaterials, *Physical Review B*, 73, 125423 (2006).
5. Z. Liu, X. Zhang, Y. Mao, Y. Zhu, Z. Yang, C.T. Chan, P. Sheng, Locally resonant sonic materials, *Science*, 289, 1734-1736 (2000).
6. N. Fang, D. Xi, J. Xu, M. Ambati, W. Srituravanich, C. Sun, X. Zhang, Ultrasonic metamaterials with negative modulus, *Nature materials*, 5, 452 (2006).
7. T. Yamamoto, Acoustic metamaterial plate embedded with Helmholtz resonators for extraordinary sound transmission loss, *Journal of Applied Physics*, 123, 215110 (2018).
8. A. Qureshi, B. Li, K. Tan, Numerical investigation of band gaps in 3D printed cantilever-in-mass metamaterials, *Scientific reports*, 6, 28314 (2016).
9. Meng, H., Chronopoulos, D., Fabro, A. T., Elmadih, W., & Maskery, I. (2020). Rainbow metamaterials for broadband multi-frequency vibration attenuation: Numerical analysis and experimental validation. *Journal of Sound and Vibration*, 465, 115005.

10. Antoniadis, I., Chronopoulos, D., Spitas, V., & Koulocheris, D. (2015). Hyper-damping properties of a stiff and stable linear oscillator with a negative stiffness element. *Journal of Sound and Vibration*, *346*, 37-52.
11. Chronopoulos, D., Antoniadis, I., & Ampatzidis, T. (2017). Enhanced acoustic insulation properties of composite metamaterials having embedded negative stiffness inclusions. *Extreme Mechanics Letters*, *12*, 48-54.
12. Chronopoulos, D., Antoniadis, I., Collet, M., & Ichchou, M. (2015). Enhancement of wave damping within metamaterials having embedded negative stiffness inclusions. *Wave Motion*, *58*, 165-179.
13. Ampatzidis, T., Leach, R. K., Tuck, C. J., & Chronopoulos, D. (2018). Band gap behaviour of optimal one-dimensional composite structures with an additive manufactured stiffener. *Composites Part B: Engineering*, *153*, 26-35.
14. Elmadih, W., Syam, W. P., Maskery, I., Chronopoulos, D., & Leach, R. (2019). Mechanical vibration bandgaps in surface-based lattices. *Additive Manufacturing*, *25*, 421-429.
15. Elmadih, W., Chronopoulos, D., Syam, W. P., Maskery, I., Meng, H., & Leach, R. K. (2019). Three-dimensional resonating metamaterials for low-frequency vibration attenuation. *Scientific reports*, 9(1), 1-8.
16. McGee, O., Jiang, H., Qian, F., Jia, Z., Wang, L., Meng, H., ... & Zuo, L. (2019). 3D printed architected hollow sphere foams with low-frequency phononic band gaps. *Additive Manufacturing*, 30, 100842.
17. Fabro, A. T., Meng, H., & Chronopoulos, D. (2020). Uncertainties in the attenuation performance of a multi-frequency metastructure from additive manufacturing. *Mechanical Systems and Signal Processing*, 138, 106557.
18. Meng, H., Chronopoulos, D., Fabro, A. T., Maskery, I., & Chen, Y. (2020). Optimal design of rainbow elastic metamaterials. *International Journal of Mechanical Sciences*, 165, 105185.